Topological Studies on IRC Paths of X + $H_2 \rightarrow XH + H$ Reactions

SHIJUN ZHENG,[1] LINGPENG MENG,[1] XINHUA CAI,[1] ZHENFENG XU,[1] XIAOYUAN FU[2]

[1]*Department of Chemistry, Hebei Teachers' College, Shijiazhuang, 050091, People's Republic of China*
[2]*Department of Chemistry, Beijing Normal University, Beijing, 100875, People's Republic of China*

Received 3 June 1996; accepted 27 November 1996

ABSTRACT: Topological properties of potential energy and electronic density distribution on five reaction paths X + $H_2 \rightarrow$ XH + H(X = H, N, HN, H_2C, NC) are investigated at the level of UMP2/6–311G(d, p). It has been found that in the region of the reaction paths studied, where $B(r_c)|_s > 0$ [$B(r_c)|_s$ is the product of $\rho(r_c)$ and $\nabla^2\rho(r_c)$ at the point of reaction process, i.e., $B(r_c)|_s = \rho(r_c)\nabla^2\rho(r_c)$] is basically the same as the region of $V''(s) < 0$[$V''(s)$ is the second derivative of potential energy with respect to the reaction coordinate, i.e., $V''(s) = d^2V/ds^2$], and the point with maximum $B(r_c)|_s$ is almost coincident with the point of minimum $V''(s)$. It can be concluded from the calculated results that there is a good correlation between the topological properties of potential energy and electronic density distribution along the reaction path. The structure transition state of such collinear reactions may be determined by topological analysis of electronic density. *J. Comput Chem* **18:** 1167–1174, 1997

Keywords: topological properties; potential energy; electronic density distribution; intrinsic reaction coordinate paths

Introduction

Topological studies of reaction paths of certain reactions have been demonstrated by various authors including ourselves some years ago.[1–3] The emphasis of these articles was on the topological properties of the chemical bonds of reactants, transition states, and products. But no one mentioned the relationship between topological characteristics of density distribution and the energy variation along the reaction path. In addition, judging the breakage or formation of a bond is almost impossible with experimental methods and traditional topological analysis. In some cases, it is known that even if two atoms A and B are a great distance apart, there is a bond path linking them. We proposed a method to determine when the bond is broken or formed. In this article, we present a topological study on the reaction processes

Correspondence to: S. J. Zheng

 CCC 0192-8651 / 97 / 091167-08

of reactions $X + H_2 \rightarrow XH + H$ (X = H, N, HN, H_2C, NC). The reaction procedures and the dynamic mechanisms of these reactions were studied experimentally and theoretically.[4–7] These radical reactions are all cooperative and are linear or quasilinear reactions. They belong to the reaction type A + B—C → A—B + C, in which an old bond B—C is broken and a new bond A—B generated. The purpose of this study is to show how chemical bonds change and when a bond is broken or formed along the reaction path by using Bader's charge density topological analysis.[8] We also discuss here the relationship between topological characteristics of density distribution and energy variation along the reaction path.

Computational Method

The geometries of various critical points on the potential energy surface were located by unrestricted Hartree–Fock calculations with second-order Møller–Plesset correlation energy corrections (UMP2), using the 6–311G(*d*, *p*) basis set. The reaction paths were traced by Fukui's theory of the intrinsic reaction coordinate (IRC).[9] Computations were performed using the HONDO7 and Gaussian 90 programs. Topological analyses were carried out with GTA-91 program, which we developed and registered at QCPE (register number QCPE-661).[10]

Results and Discussion

POTENTIAL ENERGY CURVE ON IRC PATH

Five reactions of $X + H_2 \rightarrow XH + H$ (X = H, NC, H_2C, N, HN) were studied:

(1) H + H—H → H—H—H → H—H + H

(2) N + H—H → N—H—H → N—H + H

(3)
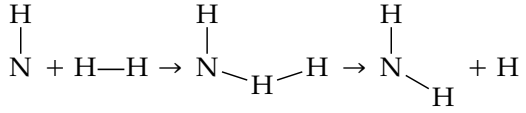

(4)
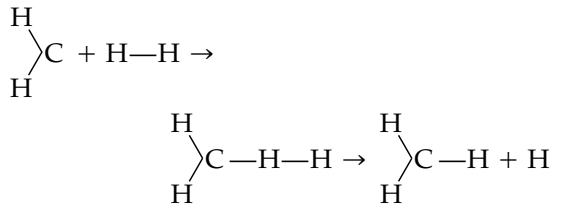

(5) N—C + H—H → N—C—H—H → N—C—H + H

Four of these reactions are linear reactions and the third one is quasilinear. The spin multiplicities in the five reactions are 2, 4, 3, 3, 2 in the above order and remain unchanged along the entire reaction path. The H—H bond is broken and X—H bond is generated in all of these reactions. The shapes of potential energy curves are depicted in Figure 1, and the potential energies are listed in Table I. From Figure 1 and Table I we can see that the product is the same as the reactant in reaction (1), so it is thermoneutral. Reactions (2) and (3) are thermonegative, while reactions (4) and (5) are thermopositive. This is because bond N—H is weaker than bond H—H, but bond C—H is stronger than bond H—H (the bond dissociation energy values of H—H, N—H, HN—H, H_2C—H, and NC—H are 0.116, 0.067, 0.087, 0.117, and 0.161 au respectively). Therefore the conclusion is that for these cooperative reactions, when a weak bond generated along with a strong bond is broken, they are endothermic; when a strong bond is generated, they are exothermic.

When the topological characteristics of the potential curves are considered, we suggest that for each potential curve there is a polynomial function between potential energy $V(s)$ and the reaction coordinate s, as follows:

$$V(s) = a_0 + a_1 s + a_2 s^2 + \cdots + a_m s^m.$$

The root-mean square minimization method is used for smoothing the potential curve with the given m ($m = 7$ for the studied reactions). It is evident that the first derivative $V'(s)$ at the point of $s = 0$ (conventional transition state) is zero. We found that the second derivatives $V''(s)$ are nega-

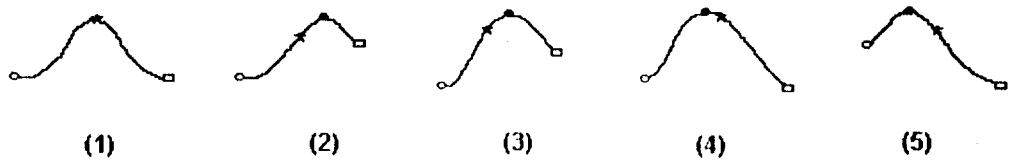

FIGURE 1. Potential energy curves for the five discussed reactions (sketch).

TABLE I.
Potential Energies on IRC Paths of Reactions.

S[a] [(amu)$^{1/2}$ bohr]	(1)	(2)	(3)	(4)	(5)
Reactant	−1.6822	−55.6531	−56.3500	−40.2919	−93.7160
…					
−0.6	6.9340	20.9478	14.8341	8.3830	1.9198
−0.5	7.9819	23.4325	16.7156	9.1537	2.1065
−0.4	9.0738	26.5133	19.0639	9.9078	2.3842
−0.3	10.2284	29.9459	21.9125	10.6594	2.7385
−0.2	11.4646	32.8448	24.6797	11.4637	3.1502
−0.1	12.4749	34.4893	26.4941	12.2106	3.1933
0.0	12.7385	34.8843	26.8939	12.6127	3.4183
0.1	12.4749	34.6521	26.7814	12.5816	2.9778
0.2	11.4646	34.1685	25.8406	11.7462	1.6804
0.3	10.2284	33.6539	24.8377	10.1639	−0.8426
0.4	9.0738	33.1464	24.4786	8.3566	−4.5003
0.5	7.9819	32.6700	23.5307	6.9012	−8.9287
0.6	6.9340	32.2368	22.7718	5.8480	−13.5391
…					
Product	0.0000	29.4002	18.5732	−0.2322	−28.0214
Barrier[b]					
+	12.7	34.9	26.9	12.6	3.4
−	12.7	5.5	8.3	12.8	31.4

The unit of the reactant energy is atomic units (au); the other energies are relative to the reactant in kcal mol^{-1}.
[a]The reaction coordinate.
[b]The unit of the barrier energy is kcal mol^{-1}; (+) forward direction and (−) backward direction of the reaction.

tive near $s = 0$ but positive elsewhere. It is interesting to consider the physical meaning of $V''(s)$. Because $V(s)$ represents energy, $V'(s)$ could be regarded as the force of driving the molecular structure change from s_i to s_j; $V''(s)$ could be considered as the vibrational frequency that indicates how the structure is changed. We might say that the molecular structure at the region where $V''(s) < 0$, near the transition state, is an imaginary-vibration structure (IVS), and the molecular structure at the region where $V''(s) > 0$ is a real-vibration structure (RVS). The point with the minimum $V''(s)$ at the region of $V''(s) < 0$ is defined as s_m. The structure at s_m and IVS will be discussed later.

TOPOLOGICAL ANALYSIS OF ELECTRONIC DENSITY ON IRC PATH

For each reaction topological analysis was carried out on the electronic density of every point along the IRC path. Topological properties are listed in Table II. The ''transition structure'' of a reaction is noted. The transition structure on the IRC path for the reaction of A—B—C → B—C—A has been discussed.[11] It is always near the (energy) transition state. In this study we performed topological analysis of electronic density ranging from $s = -0.6$ to $s = +0.6$. We found that the topological properties of bonds inside the X group exhibited little change. For example, in reaction (3), H_c—N + H_a—H_b → H_c—N—H_a + H_b, the $\rho(r_c)$ and $\nabla^2\rho(r_c)$ of the H_c—N bond at the start point, transition state, and end point of the reaction are 0.3239, −1.3955, 0.3354, −1.5368, 0.3374, and −1.5263, respectively. Here r_c is the critical point (called saddle point) on the electronic density surface, and it is connected by two gradient paths (called bond paths) from two bonded nuclei. For these linear reactions, r_c is on the axis of the system [a small deviation from the axis was found for reaction (3), a quasilinear reaction]. For convenience, we define the Laplacian function as $L(r) = -\nabla^2\rho(r)$.

According to the topological analysis of electronic density, $\rho(r_c)$ is used to describe the strength of a bond and $\nabla^2\rho(r_c)$ describes the characteristic of the bond. In general, the larger the value of $\rho(r_c)$, the stronger the bond. Where $\nabla^2\rho(r_c) < 0$, the bond is covalent. On the contrary, as $\nabla^2\rho(r_c) >$

TABLE 2.
r(r_c) and $L(r_c)$ on IRC Path of Discussed Reactions.

S	⋯	−0.6	−0.5	−.04	−0.3	−0.2	−0.1	0.0	+0.1	+0.2	+0.3	+0.4	+0.5	+0.6 ⋯
(1)														
$\rho(r_c)$	H—H ⋯	0.2540	0.2480	0.2333	0.2242	0.1999	0.1693	0.1477	0.1284	0.1042	0.0845	0.0706	0.0593	0.0502 ⋯
	X—H ⋯	0.0502	0.0593	0.0706	0.0845	0.1042	0.1284	0.1477	0.1693	0.1999	0.2242	0.2333	0.2480	0.2540 ⋯
$L(r_c)$	H—H ⋯	−1.011	−0.9633	−0.8568	−0.7933	−0.6387	−0.4622	−0.3463	−0.2460	0.1287	−0.0469	−0.0009	+0.0319	+0.0501 ⋯
	X—H ⋯	+0.0501	+0.0319	−0.0009	−0.0469	−0.1287	−0.2460	−0.3464	−0.4622	−0.6387	−0.7933	−0.8586	−0.9633	−1.001 ⋯
(2)														
$\rho(r_c)$	H—H ⋯	0.2534	0.2349	0.2055	0.1736	0.1430	0.1154	0.0937	0.0763	0.0625	0.0526	0.0450	0.0389	0.0144 ⋯
	X—H ⋯	0.0942	0.1005	0.1272	0.1501	0.1778	0.2096	0.2394	0.2665	0.2869	0.2987	0.3060	0.3110	0.3174 ⋯
$L(r_c)$	H—H ⋯	−0.9864	−0.8537	−0.6685	−0.4893	−0.3289	−0.1919	−0.0935	−0.0252	+0.0178	+0.0399	+0.0511	+0.0560	+0.0337 ⋯
	X—H ⋯	+0.1434	+0.1123	+0.0464	−0.0628	−0.2221	−0.4316	−0.6511	−0.8700	−1.051	−1.162	−1.233	−1.281	−0.1341 ⋯
(3)														
$\rho(r_c)$	H—H ⋯	0.2480	0.2349	0.2186	0.1927	0.1636	0.1352	0.1192	0.1098	0.0844	0.0684	0.0552	0.0489	0.0430 ⋯
	X—H ⋯	0.0826	0.0938	0.1086	0.1284	0.1527	0.1819	0.2008	0.2210	0.2569	0.2943	0.3091	0.3272	0.3423 ⋯
$L(r_c)$	H—H ⋯	−0.9599	−0.8669	−0.7579	−0.6010	−0.4385	−0.2891	−0.2091	−0.1400	−0.0501	+0.0105	+0.0477	+0.0551	+0.0599 ⋯
	X—H ⋯	+0.1415	+0.1224	+0.0879	+0.0182	−0.0963	−0.2613	−0.3817	−0.5185	−0.7852	−1.102	−1.414	−1.430	−1.462 ⋯
(4)														
$\rho(r_c)$	H—H ⋯	0.2456	0.2401	0.2264	0.2225	0.2065	0.1832	0.1605	0.1398	0.1162	0.0958	0.0792	0.0648	0.0541 ⋯
	X—H ⋯	0.0626	0.0694	0.0778	0.0864	0.0988	0.1152	0.1307	0.1478	0.1722	0.1983	0.2268	0.2486	0.2626 ⋯
$L(r_c)$	H—H ⋯	−0.9450	−0.9033	−0.8089	−0.7785	−0.6749	−0.5355	−0.4109	−0.3031	−0.1859	−0.0918	−0.0221	+0.0248	+0.0502 ⋯
	X—H ⋯	+0.0682	+0.0576	+0.0376	+0.0193	−0.0185	−0.0792	−0.1453	−0.2224	−0.3374	−0.4688	−0.6223	−0.7510	−0.8400 ⋯
(5)														
$\rho(r_c)$	H—H ⋯	0.2573	0.2519	0.2457	0.2309	0.2305	0.2253	0.2051	0.1778	0.1480	0.1212	0.0986	0.0804	0.0658 ⋯
	X—H ⋯	0.0499	0.0549	0.0598	0.0646	0.0726	0.0771	0.0932	0.1128	0.1329	0.1555	0.1793	0.2033	0.2276 ⋯
$L(r_c)$	H—H ⋯	−0.9400	−0.9212	−0.8951	−0.8488	−0.8050	−0.7533	−0.6430	−0.5556	−0.3962	−0.2695	−0.1591	−0.0742	−0.0134 ⋯
	X—H ⋯	+0.0905	+0.0833	+0.0722	+0.0602	+0.0433	+0.0322	+0.0021	−0.0651	−0.1485	−0.2463	−0.3597	−0.4860	−0.6266 ⋯

0 the bond belongs to the electrostatic interaction. The field of $\nabla^2\rho(r) < 0$ is a charge accumulated area and $\nabla^2\rho(r) > 0$ is a charge dispersed area. A new quantity $B(r_c) = \rho(r_c)\nabla^2\rho(r_c)$ may be defined. It is related to magnitude and characteristics of electronic density distribution. From this we can derive $B(r_c)|_s = \rho(r_c)\nabla^2\rho(r_c)|_s$, which is the value of $B(r)$ at the bond saddle point of a given reaction coordinate s. $B(r_c)|_s$ then expresses the covalent strength of the bond. It changes along with the reaction coordinate s and can be used to determine the rupture or formation of a covalent bond in such cooperative reactions. The lower the $B(r_c)|_s$, the stronger the covalent bond. When $B(r_c)|_s > 0$, the covalent bond is broken.

From calculated results, the following facts may be adduced: First, $\rho(r_c)$ of the H—H bond decreases, while the X—H bond increases as the reaction proceeds. However, the sum of $\rho(r_c)$ of the two bonds shows little variation. Minimum

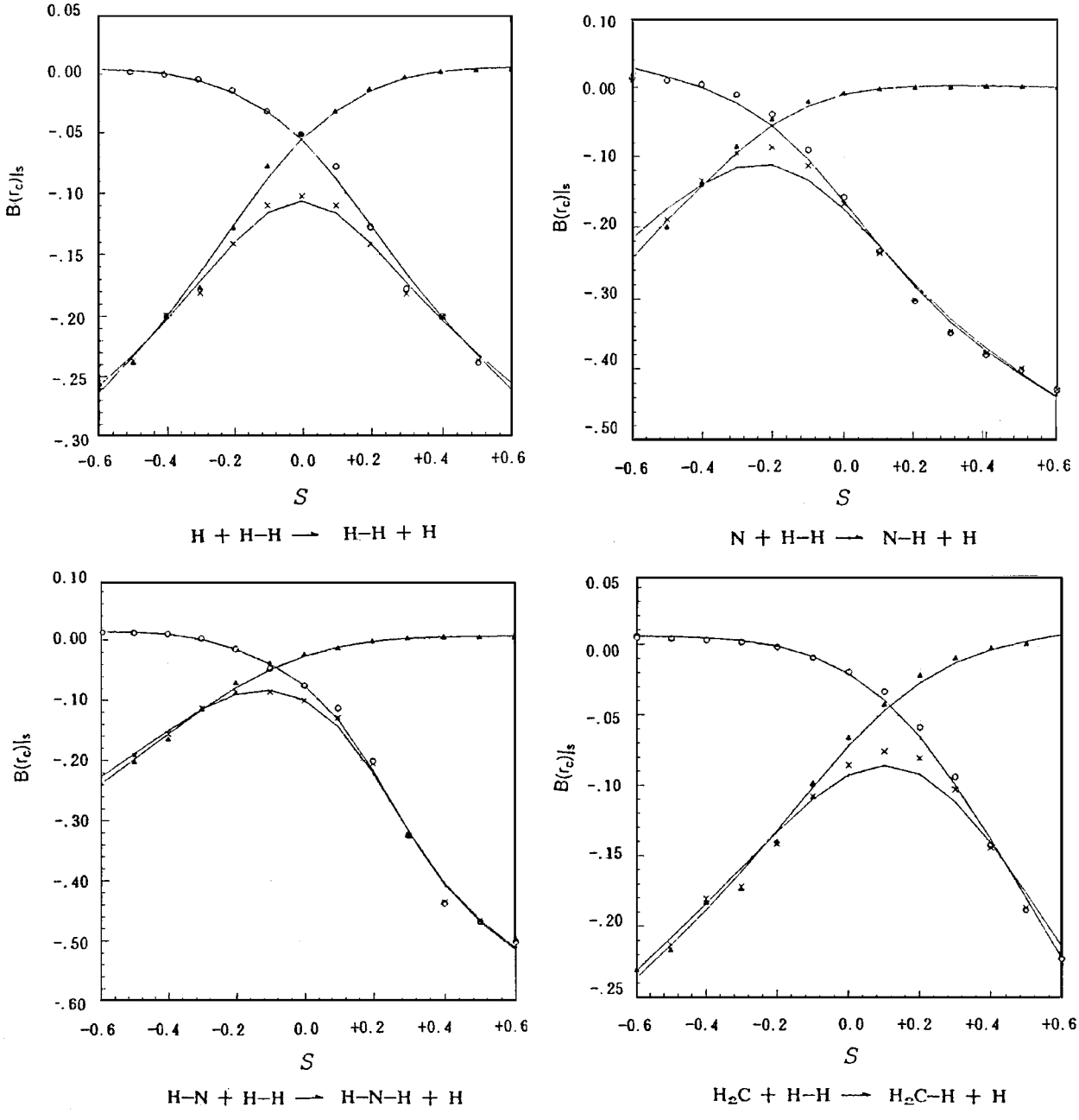

FIGURE 2. The curves of $B(r_c)|_s$. (▲) $B(r_c)|_s$ of H—H, (○) $B(r_c)|_s$ of X—H, and (×) sum of $B(r_c)|_s$.

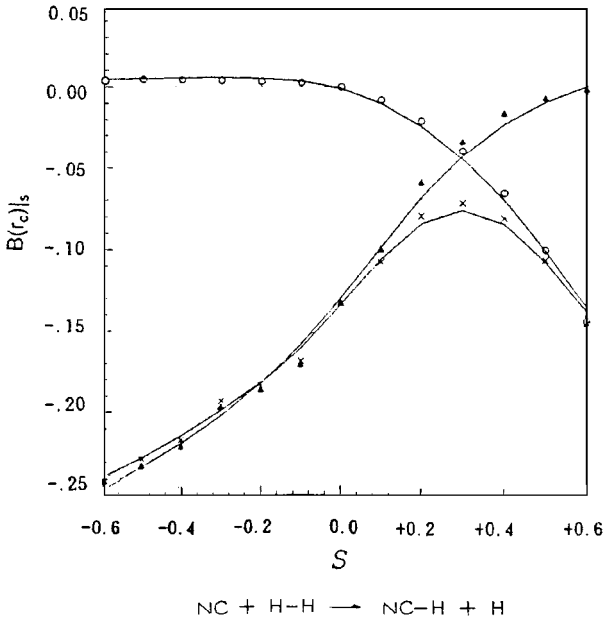

FIGURE 2. (Continued)

values of $\rho(r_c)$ appear at the point near the transition state ($s = 0$) on the IRC path. Second, $\nabla^2\rho(r_c)$ of the H—H bond increases, while that of the X—H bond decreases. A crossing point exists near the transition state ($s = 0$) on the IRC path, at which point the values of $\nabla^2\rho(r_c)$ of the two bonds are equal. There are also two points corresponding to $\nabla^2\rho(r_c) = 0$, which are not far away from the point where $s = 0$. Third, the tendency of $B(r_c)|_s$ to vary with s is similar to that of $\nabla^2\rho(r_c)|_s$. There is also a maximum $B(r_c)|_s$ near $s = 0$ on the IRC path (see Fig. 2).

Abbreviations for certain points with special meaning along the IRC path are TSP, the point of transition state; BP1, the point where $B(r_c)|_s = 0$ of H—H; BP2, the point where $B(r_c)|_s = 0$ of X—H; and BPM, the point with the maximum sum of $B(r_c)|_s$ of H—H and X—H.

It is found that BP1 occurs after TSP and BP2 occurs before TSP. But, except for reaction (1), BP1 and BP2 are always located close to TSP. As the reaction goes from start to BP1 bond X—H will be generated, and at BP2 bond H—H is broken. The narrow region from BP1 to BP2, where X—H and H—H covalent bonds coexist, we called the structure transition region. In this region the absolute value of summed $B(r_c)|_s$ (H—H + X—H) is smaller than elsewhere, and it is the smallest at BPM. This means that the combined total strength of the two bonds is the weakest at BPM. Therefore, we define the molecular structure at BPM as structure transition state (STS). For clarity, the traditional transition state is called energy transition state (ETS). STS is not always at the same point as ETS on the IRC path. We found that STS occurs before EST in endothermic reactions [reactions (2), (3)] and occurs after EST in exothermic reactions [reactions (4), (5)]. For the special case of a thermoneutral reaction [reaction (1)], STS is located at the same point as EST. In Figure 1 the STS is marked with a star on the potential curve.

For example, Figure 3 shows the contour of the $B(r_c)|_s$ of the reaction $H_2C + H—H \rightarrow H_2CH + H$. The point of $s = -0.3$ is close to BP1 and the point of $s = +0.5$ is close to BP2. The point of $s = +0.1$ is located very near to BPM. From Figure 3 we can very clearly see the breakage and formation of a chemical bond in the reaction.

RELATIONSHIP BETWEEN TOPOLOGY OF POTENTIAL ENERGY AND ELECTRONIC DENSITY

As discussed above, the potential function $V(s)$ varies with the reaction coordinate s. We found that the $V''(s)$ correlates well with $B(r_c)|_s$ (see Table III). The region where $V''(s) < 0$ coincides basically with the region of $B(r_c)|_s > 0$ on the IRC path. The point with minimum $V''(s)$ is basically the same as where maximum $B(r_c)|_s$ occurs. Its physical meaning can be understood as follows: In the region where $V''(s) < 0$, the system of reaction is at an imaginary vibration state from which the structure can transform most easily to its former or latter state. Also, in this region $B(r_c)|_s > 0$; i.e., the two covalent bonds are most easily broken or generated. Therefore, it is reasonable to call the structure in this region a transition structure. At the point with minimum $V''(s)$ and maximum $B(r_c)|_s$, the structure is at the most intense imaginary vibration state and the bonds are the most mutable. For these X + H—H → X—H + H reactions, the width of the regions as transition structures are almost the same, -0.6 (amu)$^{-1/2}\cdot$ bohr, but the width from BP1 to TSP and the width from TSP to BP2 differ among the reactions discussed here. The width of thermonegative reactions from BP1 to TSP is greater than that of thermopositive reactions, but the width from TSP to BP2 is smaller in thermonegative reactions.

Conclusions

1. The five reactions investigated are linear (or quasilinear) cooperative reactions. In each re-

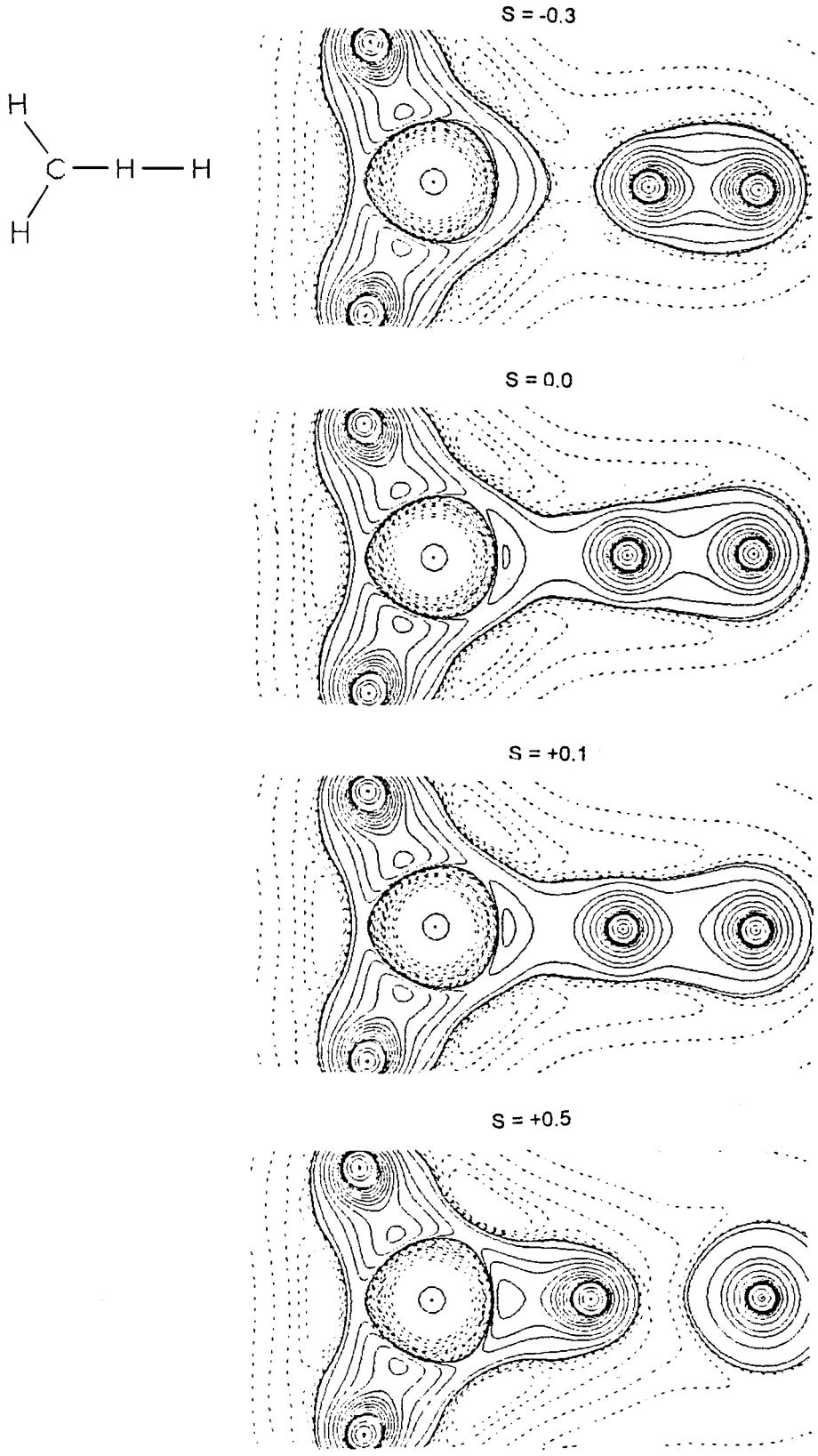

FIGURE 3. The contour of $B(r_c)|_s$ on the IRC path of the $H_2C + H—H \rightarrow H_2C—H + H$ reaction as an example. (---) positive value and (—) negative value.

TABLE III.
Comparison of Topological Properties of Potential Energy and Electronic Density

	Reaction				
	(1)	(2)	(3)	(4)	(5)
$V''(s) < 0$	−0.29 to +0.29	−0.36 to +0.16	−0.31 to +0.19	−0.26 to +0.34	−0.13 to +0.57
BP1 to BP2	−0.39 to +0.39	−0.38 to +0.16	−0.30 to +0.29	−0.21 to +0.43	−0.04 to +0.58
Minimum $V''(s)$	0.0	−0.15	−0.10	+0.13	+0.29
BPM	0.0	−0.20	−0.11	+0.15	+0.30

action only one bond is broken and one bond is generated, while the other bonds remain basically unchanged. The reaction could be described as X + A—B → X—A + B. Three centers of the reaction, X, A, and B, are linearly arranged in the reaction process.

2. The topological properties of the five reactions' potential curve show the following:
   - **a.** On the IRC path, there is a small region $[V''(s) < 0]$ where the point EST is located. In this region, imaginary vibration renders the structure of the reaction system more unstable; consequently the bonds X—H and H—H are most easily changed.
   - **b.** The minimum $V''(s)$ point on the IRC path is not the same point as EST. The structure of the reaction system at this point is the most unstable and the bonds X—H and H—H are most easily broken or generated.
3. Reaction X—A—B → A—B—X (e.g., H—C—N → C—N—H) is different from X + A—B → X—A + B. For the first one X, A, and B are nonlinear during the reaction process; it has a Δ or ⊥ type of STS at a definite point along the IRC path. But for reaction X + A—B → X—A + B, there is no such explicit point on the IRC path for the STS; there is only a small region where the reaction system exhibits transitional structure. This region can be delimited by $B(r_c)|_s > 0$. In this region we find a definite point with maximum $B(r_c)|_s$, from which the STS begin to appear.
4. There is a positive correlation between the topological property of electronic density and the topological property of the reaction potential curve. The region of $B(r_c)|_s > 0$ is almost identical with the region of $V''(s) < 0$ on the IRC path. The point having maximum $B(r_c)|_s$ coincides basically with the point having minimum $V''(s)$.
5. The STS is always near the ETS. For thermonegative reactions STS precedes EST. For thermopositive reactions STS follows EST.

References

1. X. H. Cai, L. P. Meng, and S. J. Zheng, Chem. Appl. Res. (Chinese), **2,** 91 (1990).
2. Y. Tal, R. F. W. Bader, and T. T. Nguyen−Dang, J. Chem. Phys., **74,** 5162 (1981).
3. Q. M. Li and X. Y. Fu, Acta Physico-Chim. Sinica, **8,** 724 (1992).
4. J. M. Bowman, C. Ju, and K. T. Lee, J. Phys. Chem., **86,** 2234 (1982).
5. C. D. Baskin, C. F. Bender, and C. W. Bauschlicher, J. Am. Chem. Soc. **96,** 2709 (1974).
6. R. Z. Liu, S. Y. Ma, and Z. H. Li, Acta Chim. Sinica, **52,** 1170 (1994).
7. R. A. Bair and J. H. Dunning, J. Chem. Phys., **82,** 2280 (1985).
8. R. F. W. Bader, Israel J. Chem., **19,** 8 (1980).
9. K. Ishida, K. Morokuma, and A. Komornicki, J. Chem. Phys., **66,** 2153 (1977).
10. S. J. Zheng, X. H. Cai, and L. P. Meng, QCPE Bull. **15**(2), 25 (1995).
11. R. F. W. Bader, Chem. Rev., **91,** 893 (1991).